



## Enhanced ionospheric ELF/VLF generation efficiency by multiple timescale modulated heating

G. M. Milikh<sup>1</sup> and K. Papadopoulos<sup>1</sup>

Received 30 July 2007; revised 30 August 2007; accepted 7 September 2007; published XX Month 2007.

[1] It is shown theoretically that for high power HF ionospheric heaters, such as the current HAARP heater, the HF to VLF conversion can increase significantly by using a two-timescale heating. A long heating pulse,  $t_p \approx 1$  minute, is followed over the same timescale period by modulation at the desired ELF/VLF frequency. The long pulse reduces the electron-ion recombination coefficient, resulting in increased ambient electron density and current density. The efficiency increases due to the increase in the current density over the time  $t_p$ . Besides, the more efficient heating results from sharpening of the ambient density profile at the modified height that reduces low altitude self-absorption. It is shown that following the long preheating pulse by amplitude modulated heating at VLF frequencies can result in efficiency increase of up to 7 dB over the non-preheated case. In addition to the theory the letter describes proof-of-principle experiments using the completed HAARP. **Citation:** Milikh, G. M., and K. Papadopoulos (2007), Enhanced ionospheric ELF/VLF generation efficiency by multiple timescale modulated heating, *Geophys. Res. Lett.*, *34*, LXXXXX, doi:10.1029/2007GL031518.

### 1. Introduction

[2] The generation of ELF/VLF waves by modulated heating of the lower auroral ionosphere has been the subject of numerous theoretical [Tripathi *et al.*, 1982; Papadopoulos *et al.*, 1989, 1990; Zhou *et al.*, 1996] and experimental [Barr and Stubbe, 1984, 1991; Rietveld *et al.*, 1986, 1987; Ferraro *et al.*, 1989; McCarrick *et al.*, 1990; Milikh *et al.*, 1999; Mironenko *et al.*, 1998; Papadopoulos *et al.*, 2003, 2005] investigations. A critical issue in the practical implementation of the technique is the HF to VLF conversion efficiency and its scaling with the increase in the HF power. Straightforward analysis predicts that the conversion efficiency  $\eta$  will scale at least as the square of the HF power  $P$  ( $\eta \sim P^2$ ). The scaling issue is a very opportune one since the power of the HAARP heater in Gakona, Alaska has recently increased from the level of 0.96 MW to approximately 3.6 MW. On the basis of this argument we expect that the completed HAARP facility operating at 3.6 MW power will increase the efficiency by approximately 12–14 dB. In this letter we demonstrate theoretically that by using multiple time scale heating the VLF generation efficiency can further increase by 3–7 dB thereby achieving 20 dB overall efficiency increase over the current 0.96 MW operation. In addition

to the theory the letter describes proof-of-principle experiments using the completed HAARP.

[3] Before discussing the results and the underlying physics considerations it is important to note that the methodology used to assess the efficiency is based on recent experimental results [Papadopoulos *et al.*, 2005, 2006; Rietveld *et al.*, 1987; Rietveld and Stubbe, 2006]. In this work it was demonstrated that the scaling of the conversion efficiency from HF to VLF can be assessed by studying the magnetic response of the lower ionosphere to pulsed HF heating as a function of the heating pulse length  $t_p = 1/2f$ . It was further shown by high resolution measurements [Papadopoulos *et al.*, 2005] that the waveform at a frequency  $f$  is nothing more than a superposition of the magnetic impulse responses with on-off times  $t_p = 1/2f$ . As a result the conversion efficiency for straight vertical heating can be assessed by studying the magnetic impulse response as a function of the heating pulse length.

### 2. Efficiency Enhancement Physics

[4] The physics of the efficiency enhancement at effective power level can be understood by the following simple considerations. It has been shown that to zero order the value of the magnetic field  $B$  measured on the ground scales as [Papadopoulos *et al.*, 2005]

$$B \propto j_0 S F(\Delta T_e) \quad (1)$$

where  $j_0$  is the ambient electrojet current density,  $S$  is the heated area, and  $F(\Delta T_e)$  is a function that describes the part of the conductivity modification (Hall or Pedersen) caused by the HF electron heating. Although it is not a simple linear effect, but the magnetic field  $B$  depends on the Hall and Pedersen conductance that are determined by the height profiles of the electron density. Notice that for VLF frequencies corresponding to periodic pulses with lengths shorter than few ms the electron density is essentially constant.

[5] However, this is not the case for long heating pulses. For heating times longer than tens of seconds the resultant electron heating increases the electron density by reducing the electron-ion recombination rate [Gurevich, 1978]. Since the current density, as well as the conduction scales linearly with the plasma density, preheating results in increased conversion efficiency. The density enhancement has been experimentally confirmed in artificial ionospheric modification at mid-latitudes, [e.g., Golyan *et al.*, 1982]. The temperature dependence of the recombination rate can be found by noting that the dominant positive ions in the lower ionosphere ( $z < 85$  km) are water cluster ions  $H^+(H_2O)_n$ . Their electron-ion recombination rate  $\alpha$  depends on the

<sup>1</sup>Department of Astronomy, University of Maryland, College Park, Maryland, USA.

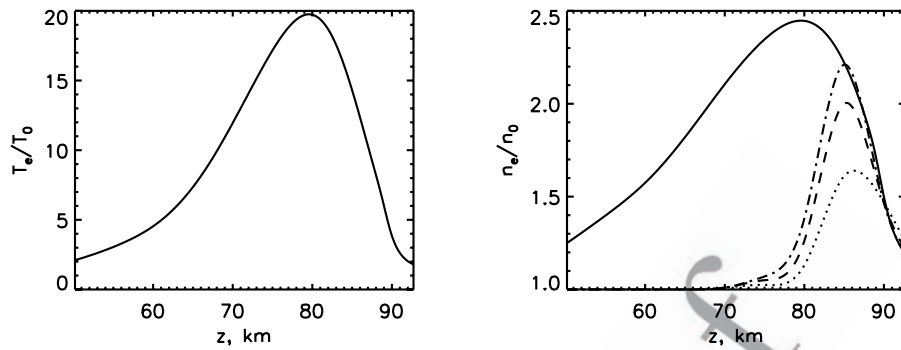


**Figure 1.** Altitude profiles of the ratio of the (left) perturbed electron temperature and (right) electron density to their respective ambient values. The heating is due to a long HF-pulse of  $f = 4$  MHz, X-mode polarization, and ERP = 88.3 dBW in the quiet nighttime auroral ionosphere. Traces from the bottom to the top on Figure 1 (right) correspond to preheating by pulse lengths of 100, 200, 300 s. The solid trace corresponds to the steady state value.

100 number of water molecules in the cluster, with an average  
101 value given by [Gurevich, 1978; Johnsen, 1993]

$$\alpha = \alpha_0(300K/T_e)^{0.6}, \quad \alpha_0 = 2.5 \times 10^{-6} \text{ cm}^3/\text{s} \quad (2)$$

103 It is important to note that while the density relaxation time  
104 is of the order of one minute the temperature relaxation time  
105 is only of the order of  $10-100 \mu\text{s}$ .

106 [6] The above considerations dictate the following strategy  
107 for efficiency enhancement using a two-timescale heating.  
108 A long heating pulse,  $t_p \approx 1$  minute, is followed over  
109 the same timescale period by modulation at the desired  
110 ELF/VLF frequency  $f \gg 1/t_p$ . The efficiency increase is the  
111 result of the increase in the current density  $j_0$  in equation (1)  
112 over the time  $T_0$  and, as shown later on, of the more  
113 efficient heating resulting from sharpening of the ambient  
114 density profile at the modified height.

115 [7] A computation of the efficiency increase by two time-  
116 scale heating requires two steps. First, we compute the  
117 density profile expected from long pulse heating as a  
118 function of the heater Effective Radiated Power (ERP),  
119 ambient ionospheric model, and pulse length. Second, we  
120 will use the modified steady density model as input in the  
121 code described by Papadopoulos *et al.* [2003, 2005] to  
122 determine the amplitude of the impulse response as a  
123 function of the short pulse length and ionospheric profile  
124 as compared to the single time-scale heating. These com-  
125 putations are presented in the next two sections.

### 126 3. Density Modification and Heating 127 Pulse-Length Requirement

128 [8] The steady state level of the modified density profile  
129 was computed in two steps: First, the Heater Code (HT)  
130 described in detail by Papadopoulos *et al.* [2003] was run to  
131 compute the steady state temperature profile. The HT code  
132 is a 1-D fluid code that models the absorption of the HF in  
133 the ionosphere, the accompanying electron heating, and the  
134 modification of the collision frequency and tensor conduc-  
135 tivity in a self-consistent manner. Inputs to the code are the  
136 electron density profile as a function of altitude, and the  
137 heater ERP, frequency, polarization, and heating pulse  
138 length. A number of ionospheric profiles similar to the ones  
139 discussed by Rietveld *et al.* [1986] are used defined by the

observed riometer absorption. Figure 1 (left) shows the  
steady state altitude profile of the electron temperature for  
the case of HF-heating at a frequency  $f_{HF} = 4$  MHz, ERP =  
88.3 dBW and X-mode polarization. This ERP level is  
consistent with HAARP heater specifications and is currently  
available. In this calculation the quiet nighttime  
ambient ionospheric density profile was used [Rietveld *et al.*,  
1986]. In this case the low altitude self-absorption is  
minimal, providing conditions for the strongest electron  
density modification. The timescale for achieving steady  
state electron temperature at the altitude of interest here  
( $<90$  km) is of the order of less than ms.

[9] Second, since the timescale for the density modifica-  
tion is of the order of one minute or longer, the density profile  
is computed by using a quasi-analytic algorithm. Namely by  
solving the ionization/recombination balance equation

$$\frac{dn_e}{dt} = q - \alpha(T_e)n_e^2, \quad (3)$$

where  $q$  is the ambient ionization rate, with the initial  
condition  $n_e(t=0) = n_0$ , and  $n_0$  is the ambient electron  
density. For  $t > 0$ , the solution of equation (3) yields

$$n_e(t) = n_0 \sqrt{\frac{\alpha_0}{\alpha_1}} \frac{(1 + \sqrt{\alpha_1/\alpha_0}) \exp\{2\sqrt{\alpha_0\alpha_1}n_0t\} - (1 - \sqrt{\alpha_1/\alpha_0})}{(1 + \sqrt{\alpha_1/\alpha_0}) \exp\{2\sqrt{\alpha_0\alpha_1}n_0t\} + (1 - \sqrt{\alpha_1/\alpha_0})}, \quad (4)$$

where  $\alpha_0 = \alpha(T_0)$ ,  $\alpha_1 = \alpha(T_1)$ . Using equation (2) the  
modified electron density profile  $n_e(z)$  is obtained for the  
pulse-width longer than the characteristic timescale of the  
electron density modification,  $\tau_{ch} = 1/\sqrt{\alpha_1\alpha_0} n_0$

$$n_e = n_0 \sqrt{\frac{\alpha_0}{\alpha_1}} \propto \left(\frac{T_e}{T_0}\right)^{0.3} \quad (5)$$

The profiles of the modified electron density corresponding  
to the parameters and ambient models used in calculating  
Figure 1 (left) are shown in the right panel of Figure 1  
computed for pulse lengths  $T_0$  of 100, 200, and 300 s.

[10] Note that the altitude of maximum density modification is determined by the two height dependent factors,  $T_e(z)$  and  $\tau_{ch}(z)$ , the latter in turn depends upon  $n_0(z)$ . As revealed by the right panel of Figure 1 at the relatively low heating time the  $n(z)$  increases at the altitudes higher than 80 km where the ambient electron density  $n_0(z)$  is large and thus the heating time  $\tau_{ch}(z)$  is short. When the heating time increases the electron density at the lower altitudes rises. Finally, under very long heating pulse the peak of electron density modification coincides with the peak of the electron temperature. Another important parameter in our analysis is the characteristic timescale required for the density to reach its steady state value as function of altitude shown as a continuous line in Figure 1 (left). The heating length required to reach .9 of its steady state value  $n_0\sqrt{\alpha_0/\alpha_1}$  is of  $\tau_{ch}$ . We computed the pulse length required to reach steady state value as a function of altitude for a quiet, nighttime ionospheric density profile. In fact, for the maximum density modification at 80 km (see Figure 1) the required pre-heating pulse lengths should be between 100–1000 s. Furthermore, since  $\tau_{ch}$  increases with decreasing altitude, pulses of the order of  $\tau_{ch}$  at 80 km will produce a sharp density profile such as shown in Figure 1, which will reduce the undesirable nonlinear absorption at the lower altitude.

#### 4. Waveforms in the Presence of Pre-heating

[11] A numerical model that describes ELF/VLF generation has been developed over past several years, and checked against observations [Papadopoulos *et al.*, 2003, 2005]. There are two steps in the computation. The first computes the spatio-temporal profile of the current density  $\vec{j}(\vec{r}, t)$  induced by the heater. This is done by using the HT heating code discussed above. The second computes the near field at the observation site, which we take as the origin of the coordinate system, by using the retarded potential method. The vector potential due to an ionospheric current which fills in the volume 2 is

$$\vec{A}(\vec{r}, t) = \frac{\mu_0}{4\pi} \int \frac{\vec{j}(\vec{r}_2, t - r_{12}/c)}{r_{12}} dV_2 \quad (6)$$

where  $\mu_0$  is permeability of free space,  $\vec{j}$  is the current density, and  $r_{12}$  is the distance between the observation point 1 and the integrated volume. Furthermore, the magnetic field generated by the current is given by

$$\vec{B}(\vec{r}, t) = \nabla \times \vec{A}(\vec{r}, t) \quad (7)$$

From these equations and assuming an ambient electric field  $E_0$  in the x direction, the Hall ( $B_x$ ) and Pedersen ( $B_y$ ) components of magnetic field at the observation point are given by

$$B_x(0, t) = \frac{\mu_0}{4\pi} SE_0 \int \left[ \frac{\Delta\sigma_H(z, t - z/c)}{z^2} + \frac{\Delta\dot{\sigma}_H(z, t - z/c)}{cz} \right] dz \quad (8)$$

$$B_y(0, t) = \frac{\mu_0}{4\pi} SE_0 \int \left[ \frac{\Delta\sigma_P(z, t - z/c)}{z^2} + \frac{\Delta\dot{\sigma}_P(z, t - z/c)}{cz} \right] dz \quad (9)$$

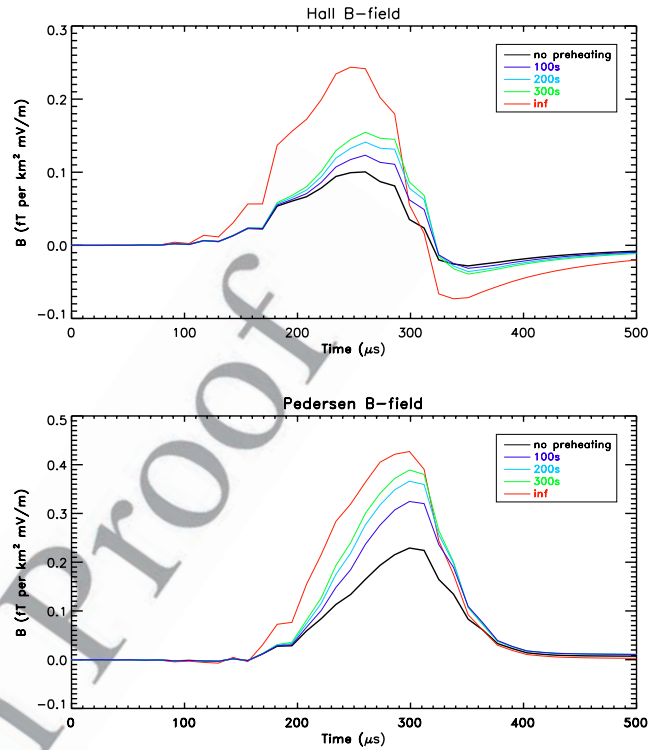


**Figure 2.** Hall and Pedersen waveforms generated by HF pulse lengths of 100  $\mu\text{s}$ ,  $f = 9.0$  MHz, ERP = 95.7 dBW, X-mode for quiet nighttime ionospheric profile. The bottom pulses correspond to the absence of preheating, while the remaining pulses by the preheating at of  $f = 4$  MHz, ERP = 88.3 dBW, X-mode and pulse lengths of 100, 200, 300 s (from the bottom to the top). The very top trace corresponds to the steady state value.

where  $\Delta\sigma_{H,P}$  are perturbations of the Hall and Pedersen 219 conductivities due to the modulated HF-heating,  $S$  is the HF 220 heated area, while  $\Delta\dot{\sigma}_{P,H}$  represents derivative with respect 221 to the retarded time. Note that the first term in the square 222 brackets in equations (8) and (9) describes the magnetic 223 field due to the ionospheric current induced by the HF 224 heating, while the second term is due to the time derivative 225 of the current. To determine the relative importance of pre- 226 heating on the efficiency of VLF generation we use the 227 following computational procedure: First use the code to 228 compute the expected VLF waveforms for ambient iono- 229 spheric profiles. Then, compute separately the modified 230 density profile due to a long pulse as discussed in Section 3. 231 Finally, rerun the code using the modified electron density 232 profile instead of the ambient one. 233

[12] Figures 2 (top) and 2 (bottom) show the Hall and 234 Pedersen magnetic field on the ground computed per unit 235 heating area and per unit electric field. They were caused by 236 a pulse of 100  $\mu\text{s}$  length, at  $f_{\text{HF}} = 9$  MHz, ERP = 95.7 dBW, 237 and X-mode polarization. The bottom plots in Figure 3 238 show the waveforms generated without preheating, while 239 the remaining plots correspond to waveforms by preheating 240 at  $f_{\text{HF}} = 4$  MHz, ERP = 88.3 dBW, X-mode with the pulse 241 lengths  $t_p = 100, 200, 300$  s. It is seen that increasing the 242 preheating pulse length results in an increase of the VLF 243 pulse that reaches maximum at the steady state value of the 244 modified profile. This effect is due to the fact that the 245

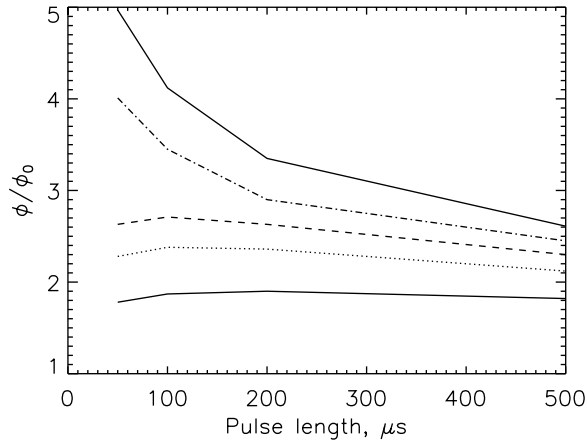


**Figure 3.** Ratio of the total magnetic flux generated by HF-pulses at 9 MHz and ERP = 95.7 dBW, X-mode for quiet nighttime ionospheric profiles, preheated by a long pulse at  $f = 4$  MHz, and ERP = 88.3 dBW, X-mode to that without preheating ( $\phi/\phi_0$ ) as a function of the short pulse length, for preheating by pulse lengths of 100, 200, 300, 500 s and by a very long pulse (from the bottom to the top respectively).

246 magnetic field on the ground scales as  $B \propto j_0 \propto n_e$  (see  
247 equation (1)). Therefore the increased electron density  
248 caused by the preheating and shown in Figure 1 leads to  
249 the respective increase in the VLF signal.

250 [13] We conducted a study by varying the heating fre-  
251 quency between the 4–9 MHz using the full HAARP ERP  
252 while keeping the preheating pulses same as above. The  
253 results indicate that the pre-heating effect optimizes at the  
254 highest HF frequency for modulated heating. It is due to the  
255 fact that the electron density modification peaks at about  
256 85 km (see Figure 1) favoring heating at high HF frequency  
257 due to the reduction of the low altitude self absorption.

258 [14] A good quantitative measure of the VLF response on  
259 the ground is the computed value of the total magnetic field  
260 flux defined as  $\phi = \int_0^{2t_p} (B_x^2 + B_y^2) dt$  where  $B_x$  and  $B_y$   
261 correspond to Hall and Pedersen components of the B-field  
262 respectively. Figure 3 shows the ratio of the total magnetic  
263 flux generated by HF-pulses at 9 MHz, ERP = 95.7 dBW,  
264 X-mode, and preheated by a long pulse of 4 MHz, ERP =  
265 88.3 dBW, X-mode, to that of a similar pulse without  
266 preheating. The computation was made for a variety of  
267 pulse lengths corresponding to VLF frequencies and for  
268 three different preheating pulse lengths. The short pulses  
269 were generated by HF at 9 MHz frequency, X-mode, and  
270 full HAARP ERP. Figure 3 indicates that the strongest  
271 increase of the magnetic flux due to preheating can reach  
272 7 dB for an infinite preheating pulse, and reduces with  
273 shorter preheating pulses. Furthermore, the effect depends  
274 upon the modulation frequency, in a fashion similar to the  
275 one discussed by *Papadopoulos et al.* [2005] in the absence  
276 of preheating. In fact, short pulses which length matches the  
277 electron heating time are more efficient in generating ELF  
278 signals than longer pulses.

## 279 5. Proof-of-Principle Experiments

280 [15] Before addressing the practical implementation of  
281 the technique and the conduct of proof-of-principle experi-

ments we should examine a role played by the transport 282  
processes in the ionosphere with respect to the ionization 283  
changes due to electron HF-heating. Taking into account the 284  
convection in the horizontal direction equation (3) can be 285  
generalized by the following way: 286

$$\frac{\partial n_e}{\partial t} + v_c \frac{\partial n_e}{\partial x} = q - \alpha n_e^2 \quad (10)$$

The convection is caused by the  $E \times B$  drift and neutral 288  
wind resulting in convection velocity given by 289

$$v_c = \sqrt{v_{dr}^2 + v_{wind}^2} + 2 \cos \theta v_{dr} v_{wind} \quad (11)$$

Here  $v_{dr}$  and  $v_{wind}$  are the  $E \times B$  drift and wind velocities 291  
respectively, while  $\theta$  is the angle between their directions. 292  
Equation (10) can be simplified by taking into account that 293  
the spatial scale of the perturbation due to HF-heating is 294  
equal to the size of the irradiated spot  $L$ , thus we get 295

$$\frac{\partial n_e}{\partial t} = q - \alpha n_e^2 - \frac{n_e v_c}{L} \quad (12)$$

[16] Equation (12) shows that the convection reduces 298  
changes in  $n_e$  due to electron heating, and increases the 299  
characteristic timescale required for the electron density to 300  
reach its steady state. In fact, the steady state density due to 301  
electron heating becomes 302

$$n_e^{st} = n_o \sqrt{\frac{\alpha_o}{\alpha}} \left\{ \sqrt{1 + \frac{1}{4\alpha q \tau_{tr}^2}} - \frac{1}{2\sqrt{\alpha q \tau_{tr}}} \right\} \quad (13)$$

where  $n_o \sqrt{\frac{\alpha_o}{\alpha}} = \sqrt{\frac{q}{\alpha}}$  is steady state density reached in the 304  
absence of the transport, while the transport timescale  $\tau_{tr} =$  305  
 $L/v_c$ . Therefore,  $n_e^{st} < n_o \sqrt{\alpha_o/\alpha}$ . Furthermore, equations (12), 306  
(13) show that the transport significantly reduces the 307  
increase in the electron density caused by HF-heating, if 308  
the transport time is shorter than the timescale required for 309  
the density to reach its steady state value  $\tau_{ch}$  shown. 310

[17] Assuming that the peak of electron perturbation 311  
occurs at about 85 km (see Figure 1 (left)) where  $\tau_{ch} \simeq$  312  
100 s, and that for the heating frequency of 4 MHz the size 313  
of spot  $L(85 \text{ km}) \simeq 30 \text{ km}$ , we obtain that the transport 314  
effect can be neglected if  $\tau_{ch} \ll \tau_{tr}$ , or if  $v_c \ll 300 \text{ m/s}$ . It 315  
means that the transport effect is negligible if the  $E \times B$  drift 316  
is caused by a moderate convection field  $E_c \ll 20 \text{ mV/m}$ . 317

[18] In the opposites case of a strong convection field 318  
( $\tau_{ch} > \tau_{tr}$ ) convection limits HF-heating time to  $\tau_{tr}$  thus 319  
reducing the peak changes in the electron density as illus- 320  
trated by Figure 1. However, the efficiency of ELF gener- 321  
ation is proportional to the value of  $E_c$ , therefore we expect 322  
that the optimal convection field of about 10 mV/m might 323  
exist although it has to be confirmed by future experiments. 324

[19] As a result, in the proposed proof-of-principles 325  
experiment the choice of preheating regime is dictated by 326  
the ionospheric conditions. At a moderate convection field, 327  
which can be detected either by the HAARP ionosonde or 328  
by radar, a long pulse of a few hundred seconds, which 329  
achieves steady state electron density, can be used for 330  
preheating. It will be followed by a modulated heating at 331

332 frequencies 1–20 kHz for a few hundred seconds. At a  
 333 strong convection field a 100–300 s preheating pulse, with  
 334 length determined by the transport time, is followed by a  
 335 modulated heating over 100–300 s at frequencies 1–20 kHz.  
 336 An alternative implementation is to split the HAARP  
 337 antenna array into two overlapping beams operating at  
 338 two different frequencies. In this case half of the power of  
 339 the array is used to maintain the modified density profile  
 340 while the remaining power is used to modulate the current.  
 341 [20] In conclusion, a novel way to increase an efficiency  
 342 of the ELF/VLF generation by HF-heating of the ionosphere  
 343 is proposed. As shown by our computer simulations a  
 344 preheating of the lower ionosphere by a long HF-pulse  
 345 can increase the peak intensity of the ELF/VLF signal by up  
 346 to 7 dB. The effect is due to increase of the local electron  
 347 density caused by a partial suppression of the electron-ion  
 348 recombination rate by the electron heating. All simulations  
 349 were made based on the characteristics of the recently  
 350 updated HAARP facility.

351 [21] **Acknowledgments.** The work was supported by the ONR Grant  
 352 NAVY.N0017302C60 and by the ONR MURI Grant 5-28828.

### 353 References

- 354 Barr, R., and P. Stubbe (1984), ELF and VLF radiation from the “polar  
 355 electrojet antenna,” *Radio Sci.*, *19*, 1111.  
 356 Barr, R., and P. Stubbe (1991), ELF radiation from the Tromsø “Super  
 357 Heater” facility, *Geophys. Res. Lett.*, *18*, 1035.  
 358 Ferraro, A. J., H. S. Lee, T. W. Collins, M. Baker, D. Werner, F. M. Zain,  
 359 and P. J. Li (1989), Measurements of extremely low frequency signals  
 360 from modulation of the polar electrojet above Fairbanks, Alaska, *IEEE*  
 361 *Trans. Antennas Propag.*, *37*, 802.  
 362 Golyan, S. F., et al. (1982), Ionization change induced in the ionospheric  
 363 E layer by intense radio waves, *Geomagn. Aeron.*, *22*, 553–555.  
 364 Gurevich, A. V. (1978), *Nonlinear Phenomena in the Ionosphere*, 370 pp.,  
 365 Springer, New York.
- Johnsen, R. (1993), Electron-temperature dependence of the recombination  
 of ions  $\text{H}_3\text{O}^+(\text{H}_2\text{O})_n$  with electrons, *J. Chem. Phys.*, *97*, 5390.  
 McCarrick, M., D. D. Sentman, A. Y. Wong, R. F. Wuerker, and B. Chouinard  
 (1990), Excitation of ELF waves in the Schuman resonance range by  
 modulated HF heating of the polar electrojet, *Radio Sci.*, *25*, 1291.  
 Milikh, G. M., K. Papadopoulos, M. McCarrick, and J. Preston (1999), ELF  
 emission generated by the HAARP HF-heater using varying frequency  
 and polarization, *Radiophys. Quantum Electr.*, *42*, 728–735.  
 Mironenko, L. F., V. O. Rapoport, S. N. Mityakov, and D. S. Kotik (1998),  
 Radiation of superluminal irregularities artificially created in the lower  
 ionosphere, *Radiophys. Quantum Electr.*, *41*, 196.  
 Papadopoulos, K., A. S. Sharma, and C. L. Chang (1989), On the efficient  
 operation of a plasma antenna driven by modulation of ionospheric cur-  
 rents, *Comments Plasma Phys. Control. Fusion*, *13*, 1.  
 Papadopoulos, K., C. L. Chang, P. Vitello, and A. Drobot (1990), On the  
 efficiency of ionospheric ELF generation, *Radio Sci.*, *25*, 1311.  
 Papadopoulos, K., T. Wallace, M. McCarrick, G. M. Milikh, and X. Yang  
 (2003), On the efficiency of ELF/VLF generation using HF heating of the  
 auroral electrojet, *Plasma Phys. Rep.*, *29*, 606–611.  
 Papadopoulos, K., T. Wallace, G. Milikh, W. Peter, and M. McCarrick  
 (2005), The magnetic response of the ionosphere to pulsed HF heating,  
*Geophys. Res. Lett.*, *32*, L13101, doi:10.1029/2005GL023185.  
 Rietveld, M. T., and P. Stubbe (2006), Comment on “The magnetic  
 response of the ionosphere to pulsed HF heating” by K. Papadopoulos  
 et al., *Geophys. Res. Lett.*, *33*, L07102, doi:10.1029/2005GL024853.  
 Rietveld, M. T., H. Kopka, and P. Stubbe (1986), D-region characteristics  
 deduced from pulsed ionospheric heating under auroral electrojet condi-  
 tions, *J. Atmos. Terr. Phys.*, *48*, 311.  
 Rietveld, M. T., P. Stubbe, and H. Kopka (1987), On the frequency depen-  
 dence of ELF/VLF waves produced by modulated ionospheric heating,  
*Radio Sci.*, *24*, 270.  
 Tripathi, V. K., C. L. Chang, and K. Papadopoulos (1982), Excitation of the  
 Earth-ionosphere waveguide by an ELF source in the ionosphere, *Radio*  
*Sci.*, *17*, 1321.  
 Zhou, H. B., K. Papadopoulos, A. S. Sharma, and C. L. Chang (1996),  
 Electromagneto-hydrodynamic response of a plasma to an external cur-  
 rent pulse, *Phys. Plasmas*, *3*, 1484.

G. M. Milikh and K. Papadopoulos, Department of Astronomy, 404  
 University of Maryland, College Park, MD 20742, USA. (milikh@astro. 405  
 umd.edu) 406